

More on the flavor dependence of m_ρ/f_π

Andrey Yu. Kotov,^a Daniel Nogradi,^b Kalman K. Szabo^{ac} and Lorinc Szikszai^b

^a*Julich Supercomputing Centre, Forschungszentrum Julich, D-52425, Germany*

^b*Eötvös University, Institute for Theoretical Physics, Budapest 1117, Hungary*

^c*Department of Physics, Wuppertal University, Gausstr. 20, D-42119, Germany*

E-mail: a.kotov@fz-juelich.de, nogradi@bodri.elte.hu,
k.szabo@fz-juelich.de, szikszai@caesar.elte.hu

ABSTRACT: In previous work, arXiv:1905.01909, we have calculated the m_ρ/f_π ratio in the chiral and continuum limit for $SU(3)$ gauge theory coupled to $N_f = 2, 3, 4, 5, 6$ fermions in the fundamental representation. The main result was that this ratio displays no statistically significant N_f -dependence. In the present work we continue the study of the N_f -dependence by extending the simulations to $N_f = 7, 8, 9, 10$. Along the way we also study in detail the N_f -dependence of finite volume effects on low energy observables and a particular translational symmetry breaking unphysical, lattice artefact phase specific to staggered fermions.

KEYWORDS: gauge theory, CFT

Contents

1	Introduction and summary	1
2	Discretization and unphysical phases with staggered fermions	2
3	Finite volume effects	4
4	Chiral-continuum extrapolation	6
5	Conclusion	9

1 Introduction and summary

We study the flavor number dependence of the ratio of the vector meson mass and the pseudoscalar decay constant in $SU(3)$ gauge theory. The ratio is significant for a large class of beyond Standard Model theories envisioning a strongly interacting Higgs sector and a composite Higgs boson [1]. The elementary fermion ingredients of the composite Higgs boson may form other bound states, such as a vector meson, which would be one of the new, so far undetected, particles the theory predicts. The pseudoscalar decay constant sets the scale, in many theories it is simply identified with $v = 246.22$ GeV, the symmetry breaking scale of the Standard Model. Having non-perturbative results for m_ρ/f_π then determines the vector meson mass m_ρ in physical units. This beyond Standard Model scenario, and variants thereof, attracted enormous interest in the lattice community in the past decade [2–34]. For a recent reviews of the available lattice results see [35] and references therein.

Apart from the phenomenological motivation the N_f -dependence of our ratio is an interesting QFT question on its own. Once both f_π and m_ρ are understood to be defined at finite fermion mass m and the chiral limit is only taken for the ratio, m_ρ/f_π is a meaningful quantity both inside and outside the conformal window. Outside the conformal window both the denominator and nominator are finite in the chiral limit with an obviously finite ratio. Inside the conformal window both m_ρ and f_π behave as $O(m^\alpha)$ for small m with the same exponent α , again leading to a finite ratio in the chiral limit. Hence the ratio is meaningful and well-defined on the full range $0 \leq N_f \leq 16$, including the quenched case $N_f = 0$ and the last integer flavor number $N_f = 16$ before asymptotic freedom is lost at $N_f = 33/2$. Formally, $N_f = 33/2$ corresponds to a free theory [36] and as such $m_\rho = 2m$ and $f_\pi = \sqrt{12}m$, leading to $m_\rho/f_\pi = 1/\sqrt{3}$. This is an order of magnitude smaller than ~ 8 found for $2 \leq N_f \leq 6$. Hence on the range $7 \leq N_f \leq 16$ the ratio will drop an order of magnitude and it is not a priori known whether the drop will be gradual or rapid, nor is it known if the onset of the conformal window somewhere around $10 \leq N_f \leq 13$ is connected to it in any way.

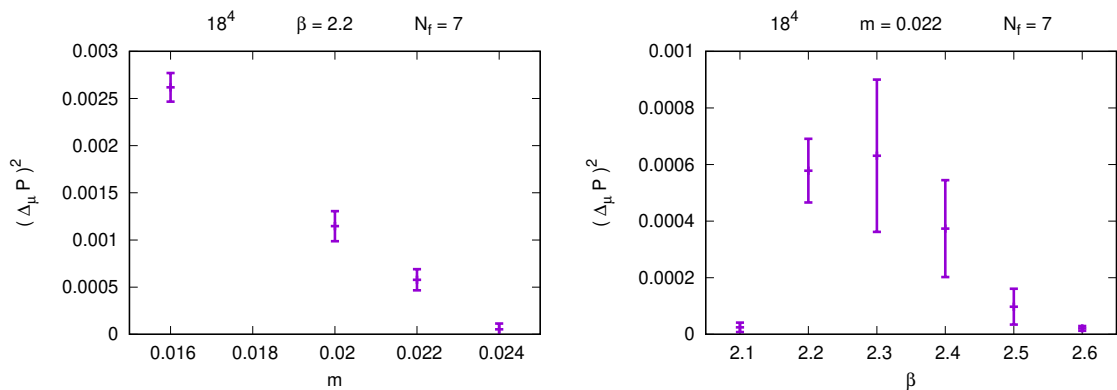


Figure 1. Two examples at $N_f = 7$ for finding the boundary of the shift symmetry broken phase. The square of the observable (2.2) is shown at fixed β (left) and fixed m (right).

Motivated by both the phenomenological implications and the purely QFT aspects we continue the investigation with $7 \leq N_f \leq 10$ in the present work. Even though we would like to know the behavior for $11 \leq N_f \leq 16$ as well, finite volume effects are growing as a function of N_f so rapidly that unfortunately we must postpone these flavor numbers to future work.

The organization of the paper is as follows. In section 2 we first study the N_f -dependence of an unphysical lattice phase specific to staggered fermions. The reason for doing so is that as N_f grows the size of the unphysical phase in the (β, m) plane grows and one must avoid it in order to perform the physically relevant chiral-continuum limit. Section 3 details our study of the finite volume effects, the upshot of which is that as N_f is growing so do finite volume effects. In fact the growth is rather rapid and is the main reason $N_f = 10$ is the highest flavor number we can reliably simulate at the moment. The chiral-continuum limit is investigated in section 4 once the bare parameters are chosen such that unphysical phases are avoided and finite volume effects are suppressed sufficiently. We end with conclusions and possible outlook to future work in section 5.

2 Discretization and unphysical phases with staggered fermions

The lattice discretization in the present work follows exactly [37]; 4 steps of stout smearing [38, 39] is applied to naive staggered fermions with smearing parameter $\varrho = 0.12$. A combination of the HMC and RHMC algorithms [40, 41] with or without rooting are used to have the desired continuum flavor number N_f .

Both in [37] and the present work simulations are run at particular points of the (β, m) phase diagram at given N_f . It is important that the bare parameters are all in the region of phase space which is continuously connected to the physical $\beta \rightarrow \infty$ region, especially because unphysical phases do exist with staggered fermions.

The possibility that in the (β, m) bare parameter space an unphysical Aoki-like phase might exist with staggered fermions was first pointed out in [42, 43]. Using staggered

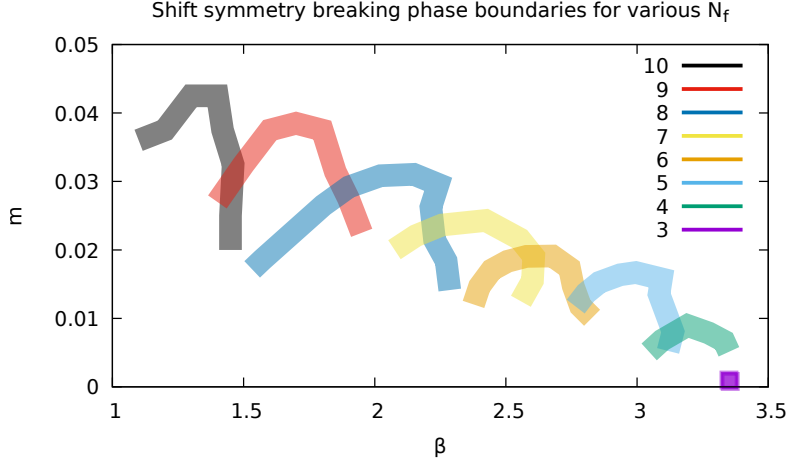


Figure 2. The shift symmetry breaking phase boundaries in the (β, m) plane. The broken phase is located under the curves, i.e. for small quark masses. The curves are given with different colors for different number of flavors.

chiral perturbation theory it was shown that decreasing the mass on coarse lattices can lead to condensation of taste split meson states which in turn means that the vacuum becomes unstable. The new vacuum has different symmetries from the one expected in the continuum and in particular the so-called staggered shift symmetry, which is a translation by a single site accompanied by a phase factor for fermion fields, is broken. Briefly, taste split meson masses M^2 in staggered chiral perturbation theory receive a continuum-like contribution from the fermion mass, $O(m)$, but also a contribution from taste splitting operators, $O(a^2)$. If the latter is negative and large in absolute value compared to the former, M^2 may turn negative, leading to the aforementioned instability. Convincing numerical evidence for this scenario was provided in [44] for $N_f = 8, 12$ and the relationship between the staggered perturbation theory picture and the actual numerical results were further clarified in [45].

In this section we study the unphysical, shift symmetry broken phase with our particular discretization and the full range of flavor numbers $2 \leq N_f \leq 10$ contained in both [37] and the present work. The main conclusion will be that even though unphysical phases do exist for $N_f > 2$ and we do map them out, our simulation points are all in the physical phase, justifying our chiral-continuum extrapolations.

The single site shift symmetry in question is [46]

$$\chi(x) \rightarrow \xi_\mu(x) \chi(x + \hat{\mu}), \quad \bar{\chi}(x) \rightarrow \bar{\chi}(x + \hat{\mu}) \xi_\mu(x), \quad U_\mu(x) \rightarrow U_\mu(x + \hat{\mu}), \quad (2.1)$$

where $\chi(x)$ is the staggered field at integer site x , $\hat{\mu}$ is the unit vector on the lattice in direction μ and $\xi_\mu(x) = (-1)^{\sum_{\nu > \mu} x_\nu}$. In this convention the staggered signs in the Dirac operator are $\eta_\mu(x) = (-1)^{\sum_{\nu < \mu} x_\nu}$. The staggered action is clearly invariant under this set of transformations.

As discussed in [44] a suitable order parameter for the study of the potential spontaneous breaking of (2.1) is the difference of plaquettes on neighboring sites. More precisely, in terms of the plaquette $P(x)$,

$$\Delta_\mu P = \sum_{x_\mu \text{ even}} \langle P(x + \hat{\mu}) - P(x) \rangle, \quad (2.2)$$

where the sum over the lattice involves only even x_μ coordinates. Clearly, if the sum would be over the entire lattice $\Delta_\mu P$ would always be zero. In this way $\Delta_\mu P$ measures if translational invariance in direction μ holds for the plaquette or not. In the physical phase, where translational invariance for gluonic observables is present, $\Delta_\mu P = 0$ for all μ . The unphysical phase will be signaled by $\Delta_\mu P \neq 0$ for at least one direction μ .

It is a straightforward exercise to map the observable $\Delta_\mu P$ as a function of (β, m) for the various flavor numbers. A useful quantity to monitor is the square $\Delta_\mu P \Delta_\mu P$ involving a sum over μ . Two typical results are shown for $\Delta_\mu P \Delta_\mu P$ at fixed β as a function of m and at fixed m as a function of β in figure 1 with $N_f = 7$ on 18^4 lattices. It is not our goal to obtain very precise values for (β_c, m_c) corresponding to the spontaneous breaking of translational invariance, for our purposes an estimate will suffice which can be read off from results of the type shown in figure 1. A detailed finite size scaling study would be required for anything more precise. As we will see our simulation points are so far away from the (β_c, m_c) phase boundaries that a rough estimate is indeed sufficient.

Performing the scans on 12^4 and 18^4 lattices shows that volume dependence is negligible on our level of precision. The summary of our results for the phase boundaries are shown in figure 2 for all flavor numbers where the thickness of the boundaries include the uncertainty related to our crude reading off of (β_c, m_c) on fixed 18^4 lattice volumes.

For each $N_f > 2$ a triangle shaped region corresponds to the spontaneously broken shift symmetry phase at finite (β, m) . This triangle presumably extends down to $m = 0$ at two particular β values. The bare mass, above which translational symmetry is unbroken for all β is a growing function of N_f as can be seen in figure 2. Not surprisingly, the particular β above which translational symmetry is unbroken for all masses is a decreasing function of N_f . At $N_f = 3$ we could not resolve the triangle shape because the broken phase only occurs for very small masses, but nevertheless could find a transition. Interestingly, we could not detect any translational symmetry broken phase for $N_f = 2$, perhaps because no such phase exists or perhaps because it occurs at extremely small masses.

The (β, m) values for $N_f = 2, 3, 4, 5, 6$ which were used in the chiral-continuum extrapolations in [37] were listed in tables 3 and 4 of said work while the same parameters are listed in table 3 for the present work with $N_f = 7, 8, 9, 10$. Clearly, all parameters used for the chiral-continuum extrapolations are in the physical phase and far from the (β_c, m_c) phase boundaries.

3 Finite volume effects

Just as in [37], a prerequisite step before chiral-continuum extrapolations are performed is the study of finite volume effects. The volume, measured in m_π units, needs to be large

N_f	β	m	L/a	am_π	af_π
7	3.00	0.0100	20	0.210(3)	0.0385(6)
			24	0.197(1)	0.0427(4)
			28	0.1913(5)	0.0434(3)
			32	0.1914(5)	0.0443(2)
			∞	0.1900(7) 2.52	0.0444(2) 1.24
8	2.68	0.0103	20	0.239(3)	0.0339(5)
			24	0.209(1)	0.0396(4)
			28	0.1999(9)	0.0415(3)
			32	0.1983(5)	0.0417(1)
			∞	0.1964(8) 0.87	0.0421(2) 0.36
9	2.49	0.0100	28	0.196(1)	0.0294(2)
			32	0.181(1)	0.0320(2)
			36	0.1771(9)	0.0329(2)
			40	0.1756(5)	0.0324(2)
			∞	0.1740(6) 0.59	0.0330(1) 6.04
10	2.30	0.0112	28	0.228(1)	0.0238(2)
			32	0.194(2)	0.0257(3)
			36	0.180(1)	0.0273(2)
			40	0.174(1)	0.0277(1)
			48	0.1704(5)	0.02813(8)
			∞	0.1699(6) 0.45	0.02807(9) 2.88

Table 1. Volume dependence of m_π and f_π and fixed lattice spacing and fermion mass, together with the infinite volume extrapolated results using (3.1) and (3.2). The χ^2/dof of the extrapolations are also shown.

enough in order to suppress finite volume distortions of the ratio m_ρ/f_π especially because as the volume is increasing m_ρ and f_π are moving in the opposite direction. The finite volume effects are thus enhancing each other in the ratio and too small volumes will lead to an overestimation of m_ρ/f_π .

An upper bound on the size of finite volume effects sets a lower bound on $m_\pi L$ for each N_f . The results in [37] have shown that this lower bound is heavily N_f -dependent in the range $2 \leq N_f \leq 6$. In the present work these finite volume investigations are extended to $7 \leq N_f \leq 10$.

The main low energy quantities m_π and f_π are measured at fixed lattice spacing and mass m for various lattice volumes, since these observables are expected to be the most sensitive to the finite volume. The $m_\pi L$ dependence of these quantities are given by

$$\begin{aligned}
m_\pi(L) &= m_{\pi\infty} + C_m g(m_{\pi\infty}L) \\
f_\pi(L) &= f_{\pi\infty} - C_f g(m_{\pi\infty}L) ,
\end{aligned}
\tag{3.1}$$

with some $m_{\pi\infty}$, $f_{\pi\infty}$, C_m and C_f parameters. The details follow the procedure explained in [37], in particular we have

$$g(x) = \frac{4}{x} \sum_{n \neq 0} \frac{K_1(nx)}{n}
\tag{3.2}$$

in terms of the Bessel function K_1 . The sum is over integers (n_1, n_2, n_3, n_4) with $n^2 = n_1^2 + n_2^2 + n_3^2 + 4n_4^2 \neq 0$ where $\mu = 4$ corresponds to the time direction. The function $g(x)$ describing the finite volume effects represents the lightest particle, the pion, going around the finite volume in all 3 space and the time direction any number of times. The leading contribution for our geometry, where the lattice is largest in the time direction comes from the pion going around each spatial direction once, corresponding to $n = (\pm 1, 0, 0, 0), (0, \pm 1, 0, 0), (0, 0, \pm 1, 0)$. If only these terms are kept we are led to the familiar finite volume effects given by a single exponential,

$$g(x) = 24\sqrt{\frac{\pi}{2}} \frac{e^{-x}}{x^{3/2}} \left(1 + O\left(\frac{1}{x}\right)\right) + O\left(e^{-\sqrt{2}x}\right). \quad (3.3)$$

We have repeated the finite volume fits with the above leading order single exponential expression as well and the results did not change within statistical uncertainties hence the data can not distinguish between the two sets of extrapolations. Note that the finite volume extrapolations (3.1) with either (3.2) or (3.3) do not depend on chiral perturbation theory at all, they hold for any massive QFT with m_π taking the place of the lightest mass. In particular even if N_f is inside the conformal window but a finite mass is introduced leading to finite masses for physical excitations, finite volume effects are still described by (3.1) and (3.2) or approximately (3.3).

The results of our fits of the type (3.1) with (3.2) are shown in figure 3.

The main conclusion from the finite volume volume study is that as N_f is increasing the minimal $m_\pi L$ required for at most 1% finite volume effects needs to grow. On the full range $2 \leq N_f \leq 10$ including the results from [37] the bounds can be interpolated by the simple expression,

$$m_\pi L > 3.46 + 0.12N_f + 0.03N_f^2. \quad (3.4)$$

For instance at $N_f = 10$ we have $m_\pi L > 7.66$, about twice as large as the corresponding bound at $N_f = 2$.

Apart from the exponential finite volume effects discussed above for f_π and m_π , there might be further finite volume effects influencing m_ϱ because of its possible decay to 2 pions. For our simulation points ϱ is however stable.

The conclusion from this section is that our simulation results suffer from at most 1% finite volume effects for $N_f = 7, 8, 9$ and at most 1.5% for $N_f = 10$, resulting in at most 3% distortion in the ratio m_ϱ/f_π , well below our statistical uncertainties.

4 Chiral-continuum extrapolation

Apart from the observables m_π, f_π and m_ϱ the gradient flow scale t_0 was also measured to set the scale in the chiral-continuum extrapolations. The right hand side in the definition of t_0 [47],

$$\langle t_0^2 E(t_0) \rangle = c \quad (4.1)$$

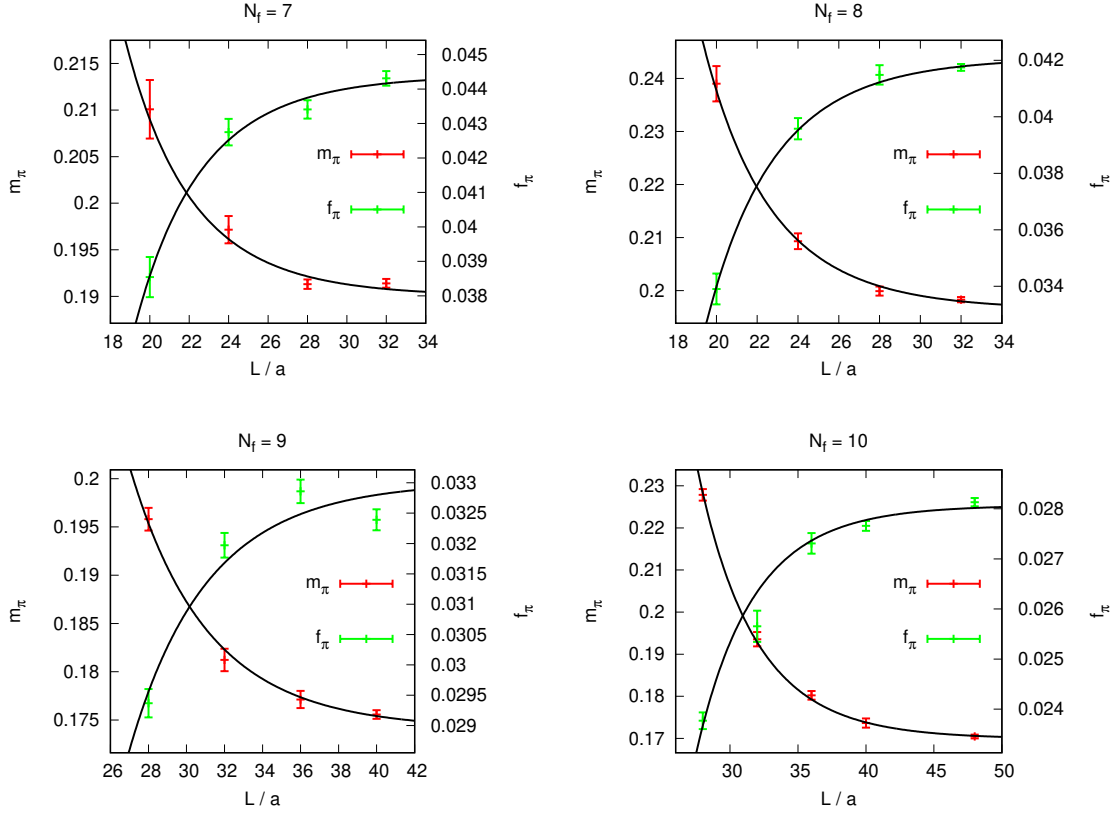


Figure 3. Finite volume effects for m_π and f_π for all flavors $7 \leq N_f \leq 10$. Extrapolations are via (3.2) and the data is tabulated in table 1.

is in principle arbitrary, in QCD usually $c = 0.3$ is used. It is possible to choose different $c = c(N_f)$ for different N_f though. A combination of cut-off effects, statistical uncertainty and computational resources led to our following choices $c(7) = 0.45$, $c(8) = 0.45$, $c(9) = 0.40$, $c(10) = 0.32$.

Once t_0 is measured along with our low energy quantities of interest the chiral-continuum extrapolation is performed via

$$X\sqrt{t_0} = C_0 + C_1 m_\pi^2 t_0 + C_2 \frac{a^2}{t_0} + C_3 \frac{a^2}{t_0} m_\pi^2 t_0, \quad (4.2)$$

where $X = f_\pi$ or m_π . The continuum mass dependence is given by $C_0 + C_1 m_\pi^2 t_0$ and the two terms C_2 and C_3 parametrize cut-off effects in both the chiral limit value C_0 and the slope C_1 .

The measured data for $m_\pi, f_\pi, m_\rho, t_0$ are shown in figure 3. The lattice geometry was always $L^3 \times 2L$, the collected number of thermalized configurations $O(1000)$ and every 10^{th} was used for measurements. For each flavor number, simulations are performed at 3 lattice spacings with 4 masses at each. Hence the chiral-continuum extrapolations (4.2) correspond to $dof = 8$ in each case.

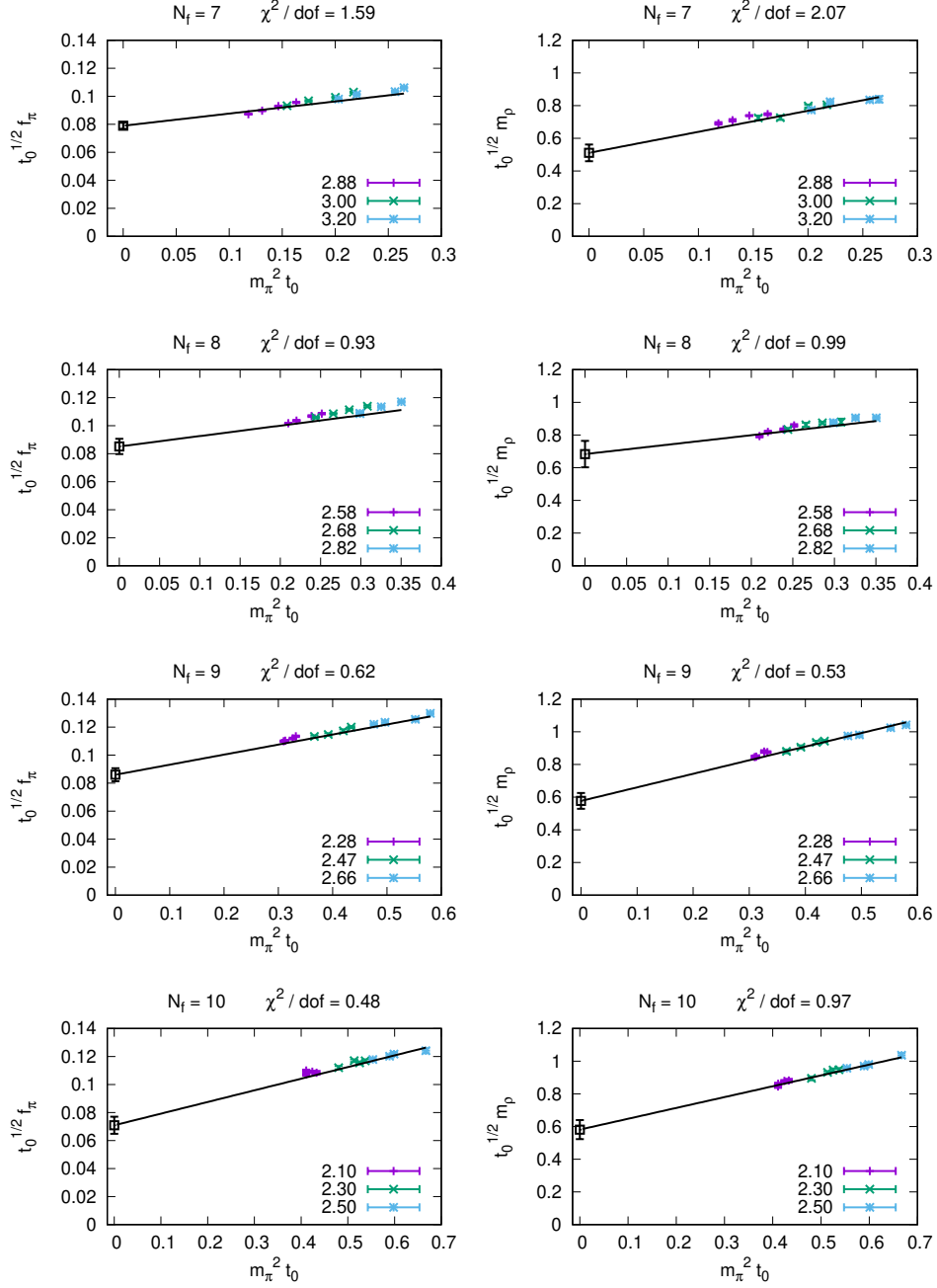


Figure 4. Chiral-continuum extrapolation of f_π and m_ρ in t_0 units using the 4-parameter global fit (4.2). The χ^2/dof of the extrapolation is also shown. The solid black line corresponds to the resulting continuum mass dependence $C_0 + C_1 m_\pi^2 t_0$, i.e. dropping C_2 and C_3 which are responsible for the cut-off effects. The deviations from the data at given bare coupling β shown by different colors, and the straight line are indicative of said cut-off effects. The absolute scale on the axis can not be directly compared between different flavor numbers because the definition of t_0 was N_f -dependent, see (4.1).

N_f	$f_\pi\sqrt{t_0}$	$m_\varrho\sqrt{t_0}$	m_ϱ/f_π
7	0.079(2)	0.51(5)	6.5(7)
8	0.085(5)	0.68(8)	8.0(1.1)
9	0.086(5)	0.58(5)	6.7(7)
10	0.071(6)	0.58(6)	8.2(1.1)

Table 2. Continuum results for each N_f in the chiral limit.

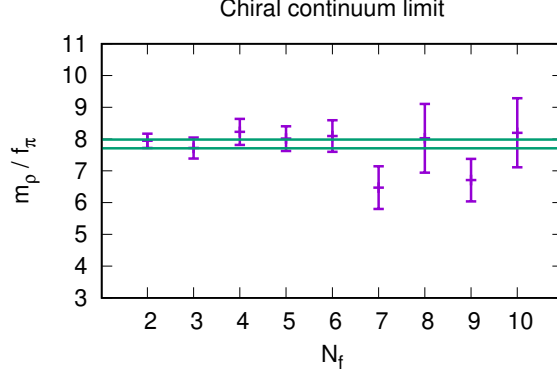


Figure 5. The N_f -dependence of m_ϱ/f_π in the chiral-continuum limit. The results with $2 \leq N_f \leq 6$ are from [37] and $7 \leq N_f \leq 10$ corresponds to this work. The result of a constant fit as a function of N_f is also shown.

The chiral-continuum extrapolations are shown in figure 4 and the results are tabulated in table 2. The full N_f -dependence of m_ϱ/f_π in the chiral-continuum limit for $2 \leq N_f \leq 10$ using also the results from [37] is shown in figure 5.

It was observed in [37] that there is no statistically significant N_f -dependence in the ratio for $2 \leq N_f \leq 6$, at least on the level of precision available there. A statistically good constant fit gave $m_\varrho/f_\pi = 7.95(15)$. We can now repeat the constant fit on the new range $7 \leq N_f \leq 10$ and the result is $m_\varrho/f_\pi = 7.01(40)$ with $\chi^2/dof = 0.97$, which represents a slight 2σ -decrease. Nevertheless combining all results on the full range $2 \leq N_f \leq 10$ we obtain $m_\varrho/f_\pi = 7.85(14)$ with $\chi^2/dof = 1.10$ which is our final result.¹ Apparently, the free value $m_\varrho/f_\pi = 1/\sqrt{3}$ at $N_f = 33/2$ is still about an order of magnitude away.

5 Conclusion

In this work we continued our study of the ratio m_ϱ/f_π in the chiral-continuum limit. Constant fits as a function of N_f on the two ranges $2 \leq N_f \leq 6$ and $7 \leq N_f \leq 10$ show

¹As a consistency check we have also fitted the N_f -dependence as $m_\varrho/f_\pi = A + N_f B$ which resulted in $A = 8.17(29)$, $B = -0.083(66)$ with $\chi^2/dof = 1.04$. The fit parameter B is consistent with zero on the 1.3σ level.

a decrease on the 2σ -level but a constant fit on the full range $2 \leq N_f \leq 10$ is still a statistically acceptable result and leads to $m_\rho/f_\pi = 7.85(14)$.

The main conclusion is the reinforcement of the picture arising from [37], namely that m_ρ/f_π is a robust quantity once the gauge group is fixed and does not depend much, if at all, on the fermion content. Applied to composite Higgs models inspired by strong dynamics, this would mean that a potential measurement of a new so far unobserved vector resonance inherent in these types of models, would not select the flavor number. The measured vector mass would rather place constraints on the gauge group [48].

Our ratio has a well-defined meaning in the chiral limit both inside and outside the conformal window. If the free value $m_\rho/f_\pi = 1/\sqrt{3} = 0.577$ is to be reached at $N_f = 16.5$, an order of magnitude drop ought to take place beyond $N_f = 10$. If the trends of finite volume effects follow (3.4) in any sense, the $N_f > 10$ simulations will be very challenging. It would be most interesting to work out the perturbative corrections to $1/\sqrt{3}$ close to the upper end of the conformal window, i.e. not much below $N_f = 16.5$ where perturbation theory is reliable. Hopefully the full range $2 \leq N_f \leq 16$ can then be covered by a combination of non-perturbative simulations and perturbative results. The onset of the conformal window would probably leave some sort of imprint on the flavor dependence of the ratio, a subject we leave for future work.

Acknowledgements

DN would like to thank very useful discussions with Stephan Durr and Sandor Katz. The simulations were carried out on the GPU clusters of Eotvos University Budapest and University of Wuppertal and at HLRS in Stuttgart, Germany. This work was in part supported by the Hungarian National Research, Development and Innovation Office (NKFIH) grant KKP126769.

References

- [1] W. A. Bardeen, C. T. Hill and M. Lindner, Phys. Rev. D **41**, 1647 (1990)
- [2] Z. Fodor, K. Holland, J. Kuti, D. Nogradi and C. Schroeder, Phys. Lett. B **681**, 353-361 (2009) [arXiv:0907.4562 [hep-lat]].
- [3] L. Del Debbio, B. Lucini, A. Patella, C. Pica and A. Rago, Phys. Rev. D **82**, 014509 (2010) [arXiv:1004.3197 [hep-lat]].
- [4] L. Del Debbio, B. Lucini, A. Patella, C. Pica and A. Rago, Phys. Rev. D **82**, 014510 (2010) [arXiv:1004.3206 [hep-lat]].
- [5] F. Bursa, L. Del Debbio, D. Henty, E. Kerrane, B. Lucini, A. Patella, C. Pica, T. Pickup and A. Rago, Phys. Rev. D **84**, 034506 (2011) [arXiv:1104.4301 [hep-lat]].
- [6] Z. Fodor, K. Holland, J. Kuti, D. Nogradi, C. Schroeder and C. H. Wong, Phys. Lett. B **718**, 657-666 (2012) [arXiv:1209.0391 [hep-lat]].
- [7] T. Appelquist, R. C. Brower, M. I. Buchoff, M. Cheng, G. T. Fleming, J. Kiskis, M. F. Lin, E. T. Neil, J. C. Osborn and C. Rebbi, *et al.* Phys. Rev. Lett. **112**, no.11, 111601 (2014) [arXiv:1311.4889 [hep-ph]].
- [8] Y. Aoki *et al.* [LatKMI], Phys. Rev. Lett. **111**, no.16, 162001 (2013) [arXiv:1305.6006 [hep-lat]].

- [9] A. Hietanen, R. Lewis, C. Pica and F. Sannino, JHEP **07**, 116 (2014) [arXiv:1404.2794 [hep-lat]].
- [10] T. Appelquist *et al.* [LSD], Phys. Rev. D **90**, no.11, 114502 (2014) [arXiv:1405.4752 [hep-lat]].
- [11] Y. Aoki *et al.* [LatKMI], Phys. Rev. D **89**, 111502 (2014) [arXiv:1403.5000 [hep-lat]].
- [12] Y. Aoki *et al.* [LatKmi], Int. J. Mod. Phys. A **32**, no.35, 1747010 (2017) [arXiv:1510.07373 [hep-lat]].
- [13] T. DeGrand, Y. Liu, E. T. Neil, Y. Shamir and B. Svetitsky, Phys. Rev. D **91**, 114502 (2015) [arXiv:1501.05665 [hep-lat]].
- [14] L. Del Debbio, B. Lucini, A. Patella, C. Pica and A. Rago, Phys. Rev. D **93**, no.5, 054505 (2016) [arXiv:1512.08242 [hep-lat]].
- [15] Y. Aoki *et al.* [LatKMI], Phys. Rev. D **96**, no.1, 014508 (2017) [arXiv:1610.07011 [hep-lat]].
- [16] T. Appelquist, R. C. Brower, G. T. Fleming, A. Hasenfratz, X. Y. Jin, J. Kiskis, E. T. Neil, J. C. Osborn, C. Rebbi and E. Rinaldi, *et al.* Phys. Rev. D **93**, no.11, 114514 (2016) [arXiv:1601.04027 [hep-lat]].
- [17] Z. Fodor, K. Holland, J. Kuti, S. Mondal, D. Negradi and C. H. Wong, Phys. Rev. D **94**, no.1, 014503 (2016) [arXiv:1601.03302 [hep-lat]].
- [18] T. A. DeGrand, M. Golterman, W. I. Jay, E. T. Neil, Y. Shamir and B. Svetitsky, Phys. Rev. D **94**, no.5, 054501 (2016) [arXiv:1606.02695 [hep-lat]].
- [19] R. Arthur, V. Drach, M. Hansen, A. Hietanen, C. Pica and F. Sannino, Phys. Rev. D **94**, no.9, 094507 (2016) [arXiv:1602.06559 [hep-lat]].
- [20] Z. Fodor, K. Holland, J. Kuti, S. Mondal, D. Negradi and C. H. Wong, Phys. Rev. D **94**, no.9, 091501 (2016) [arXiv:1607.06121 [hep-lat]].
- [21] T. Appelquist, J. Ingoldby and M. Piai, JHEP **03**, 039 (2018) [arXiv:1711.00067 [hep-ph]].
- [22] T. Appelquist, J. Ingoldby and M. Piai, JHEP **07**, 035 (2017) [arXiv:1702.04410 [hep-ph]].
- [23] V. Ayyar, T. DeGrand, M. Golterman, D. C. Hackett, W. I. Jay, E. T. Neil, Y. Shamir and B. Svetitsky, Phys. Rev. D **97**, no.7, 074505 (2018) [arXiv:1710.00806 [hep-lat]].
- [24] L. Del Debbio, C. Englert and R. Zwicky, JHEP **08**, 142 (2017) [arXiv:1703.06064 [hep-ph]].
- [25] T. Appelquist *et al.* [Lattice Strong Dynamics], Phys. Rev. D **99**, no.1, 014509 (2019) [arXiv:1807.08411 [hep-lat]].
- [26] V. Ayyar, T. DeGrand, D. C. Hackett, W. I. Jay, E. T. Neil, Y. Shamir and B. Svetitsky, Phys. Rev. D **99**, no.9, 094502 (2019) [arXiv:1812.02727 [hep-ph]].
- [27] V. Ayyar, T. Degrand, D. C. Hackett, W. I. Jay, E. T. Neil, Y. Shamir and B. Svetitsky, Phys. Rev. D **97**, no.11, 114505 (2018) [arXiv:1801.05809 [hep-ph]].
- [28] T. Appelquist, J. Ingoldby and M. Piai, Phys. Rev. D **101**, no.7, 075025 (2020) [arXiv:1908.00895 [hep-ph]].
- [29] Z. Fodor, K. Holland, J. Kuti and C. H. Wong, PoS **LATTICE2018**, 196 (2019) [arXiv:1901.06324 [hep-lat]].
- [30] R. C. Brower *et al.* [USQCD], Eur. Phys. J. A **55**, no.11, 198 (2019) [arXiv:1904.09964 [hep-lat]].
- [31] V. Ayyar, M. F. Golterman, D. C. Hackett, W. Jay, E. T. Neil, Y. Shamir and B. Svetitsky, Phys. Rev. D **99**, no.9, 094504 (2019) [arXiv:1903.02535 [hep-lat]].
- [32] Z. Fodor, K. Holland, J. Kuti and C. H. Wong, PoS **LATTICE2019**, 246 (2020) [arXiv:2002.05163 [hep-lat]].
- [33] T. Appelquist *et al.* [Lattice Strong Dynamics], Phys. Rev. D **103**, no.1, 014504 (2021) [arXiv:2007.01810 [hep-ph]].

- [34] A. Hasenfratz, C. Rebbi and O. Witzel, Phys. Rev. D **101**, no.11, 114508 (2020) [arXiv:2004.00754 [hep-lat]].
- [35] V. Drach, PoS **LATTICE2019**, 242 (2020) [arXiv:2005.01002 [hep-lat]].
- [36] K. Cichy, J. Gonzalez Lopez, K. Jansen, A. Kujawa and A. Shindler, Nucl. Phys. B **800**, 94-108 (2008) [arXiv:0802.3637 [hep-lat]].
- [37] D. Nogradi and L. Szikszai, JHEP **05**, 197 (2019) [arXiv:1905.01909 [hep-lat]].
- [38] C. Morningstar and M. J. Peardon, Phys. Rev. D **69**, 054501 (2004) [arXiv:hep-lat/0311018 [hep-lat]].
- [39] S. Durr, Z. Fodor, C. Hoelbling, S. D. Katz, S. Krieg, T. Kurth, L. Lellouch, T. Lippert, K. K. Szabo and G. Vulvert, JHEP **08**, 148 (2011) [arXiv:1011.2711 [hep-lat]].
- [40] S. Duane, A. D. Kennedy, B. J. Pendleton and D. Roweth, Phys. Lett. B **195**, 216-222 (1987)
- [41] M. A. Clark and A. D. Kennedy, Phys. Rev. Lett. **98**, 051601 (2007) [arXiv:hep-lat/0608015 [hep-lat]].
- [42] W. J. Lee and S. R. Sharpe, Phys. Rev. D **60**, 114503 (1999) [arXiv:hep-lat/9905023 [hep-lat]].
- [43] C. Aubin and Q. h. Wang, Phys. Rev. D **70**, 114504 (2004) [arXiv:hep-lat/0410020 [hep-lat]].
- [44] A. Cheng, A. Hasenfratz and D. Schaich, Phys. Rev. D **85**, 094509 (2012) [arXiv:1111.2317 [hep-lat]].
- [45] C. Aubin, K. Colletti and G. Davila, Phys. Rev. D **93**, no.8, 085009 (2016) [arXiv:1512.01254 [hep-lat]].
- [46] M. F. L. Golterman and J. Smit, Nucl. Phys. B **245**, 61-88 (1984)
- [47] M. Lüscher, JHEP **08**, 071 (2010) [erratum: JHEP **03**, 092 (2014)] [arXiv:1006.4518 [hep-lat]].
- [48] D. Nogradi and L. Szikszai, PoS **LATTICE2019**, 237 (2019) [arXiv:1912.04114 [hep-lat]].

N_f	β	m	L/a	am_π	af_π	am_ρ	t_0/a^2	$m_\pi L$	$f_\pi L$
7	2.88	0.0149	24	0.2583(5)	0.0612(2)	0.478(3)	2.45(2)	6.20(1)	1.469(5)
		0.0122	28	0.2327(4)	0.0565(1)	0.449(2)	2.70(2)	6.52(1)	1.583(4)
		0.0100	28	0.2092(4)	0.0519(1)	0.410(4)	2.99(2)	5.86(1)	1.452(4)
		0.0086	32	0.1932(4)	0.04904(9)	0.389(4)	3.17(2)	6.18(1)	1.569(3)
	3.00	0.0147	28	0.2353(8)	0.0520(2)	0.406(3)	3.92(2)	6.59(2)	1.455(4)
		0.0125	28	0.2164(4)	0.0480(2)	0.386(4)	4.28(4)	6.06(1)	1.345(4)
		0.0100	32	0.1914(5)	0.0443(2)	0.333(6)	4.77(3)	6.12(2)	1.418(7)
		0.0084	36	0.1738(5)	0.0412(1)	0.320(6)	5.12(3)	6.26(2)	1.484(5)
	3.20	0.0115	36	0.1741(6)	0.0359(2)	0.284(6)	8.74(6)	6.27(2)	1.292(6)
		0.0100	36	0.1630(8)	0.0333(2)	0.269(4)	9.65(6)	5.87(3)	1.198(7)
		0.0085	40	0.1479(3)	0.0319(2)	0.260(4)	10.07(9)	5.92(1)	1.277(7)
		0.0077	40	0.1403(5)	0.0305(2)	0.241(3)	10.3(1)	5.61(2)	1.219(7)
8	2.58	0.0149	24	0.2619(5)	0.0567(2)	0.448(4)	3.67(3)	6.28(1)	1.361(5)
		0.0124	28	0.2355(5)	0.0515(2)	0.402(2)	4.30(5)	6.59(1)	1.442(4)
		0.0099	28	0.2096(8)	0.0463(1)	0.366(3)	5.01(5)	5.87(2)	1.296(4)
		0.0087	32	0.1945(5)	0.0432(1)	0.337(3)	5.55(3)	6.23(2)	1.383(4)
	2.68	0.0145	28	0.2400(7)	0.0492(2)	0.380(8)	5.35(5)	6.72(2)	1.378(5)
		0.0124	28	0.2207(6)	0.0460(2)	0.361(2)	5.86(6)	6.18(2)	1.288(4)
		0.0103	32	0.1983(5)	0.0417(1)	0.332(4)	6.76(5)	6.34(2)	1.336(4)
		0.0083	36	0.1750(5)	0.0375(1)	0.296(3)	7.97(7)	6.30(2)	1.350(4)
	2.82	0.0120	36	0.1959(6)	0.0387(2)	0.300(3)	9.13(8)	7.05(2)	1.394(6)
		0.0100	36	0.1770(5)	0.0352(1)	0.281(3)	10.4(1)	6.37(2)	1.269(5)
		0.0080	36	0.1583(6)	0.0314(3)	0.253(4)	11.9(2)	5.70(2)	1.132(9)
		0.0075	40	0.1515(5)	0.0302(1)	0.243(2)	13.0(1)	6.06(2)	1.207(5)
9	2.28	0.0164	28	0.2672(5)	0.0526(2)	0.406(2)	4.66(4)	7.48(1)	1.472(4)
		0.0128	32	0.2311(5)	0.0452(1)	0.355(3)	6.12(6)	7.39(2)	1.447(4)
		0.0100	36	0.1994(3)	0.0393(1)	0.302(3)	7.86(9)	7.18(1)	1.416(4)
		0.0090	40	0.1875(2)	0.03703(9)	0.285(3)	8.81(7)	7.500(9)	1.481(4)
	2.47	0.0140	32	0.2198(5)	0.0400(1)	0.315(2)	8.98(8)	7.03(2)	1.281(4)
		0.0110	36	0.1906(5)	0.0345(2)	0.275(2)	11.5(2)	6.86(2)	1.243(6)
		0.0090	40	0.1684(6)	0.0309(2)	0.244(2)	13.8(2)	6.74(2)	1.234(7)
		0.0070	48	0.1442(3)	0.0270(1)	0.210(2)	17.6(2)	6.92(2)	1.296(5)
	2.66	0.0200	28	0.248(1)	0.0423(2)	0.340(1)	9.4(1)	6.95(3)	1.185(7)
		0.0150	32	0.2078(7)	0.0351(2)	0.287(2)	12.8(2)	6.65(2)	1.124(7)
		0.0120	40	0.1785(8)	0.0313(2)	0.249(2)	15.6(3)	7.14(3)	1.250(7)
		0.0098	48	0.1568(5)	0.0277(2)	0.222(2)	19.3(2)	7.53(2)	1.331(7)
10	2.10	0.0165	32	0.2423(7)	0.0416(2)	0.326(2)	7.00(7)	7.75(2)	1.330(5)
		0.0126	36	0.2037(7)	0.0342(1)	0.275(1)	10.2(1)	7.33(2)	1.230(5)
		0.0100	40	0.1801(9)	0.0297(2)	0.241(2)	13.4(3)	7.20(3)	1.186(6)
		0.0081	48	0.1535(6)	0.02567(9)	0.202(2)	17.4(2)	7.37(3)	1.232(4)
	2.30	0.0185	32	0.2386(7)	0.0390(1)	0.310(1)	9.0(1)	7.63(2)	1.247(5)
		0.0142	36	0.2005(9)	0.0320(1)	0.259(2)	13.4(2)	7.22(3)	1.152(5)
		0.0112	40	0.174(1)	0.0277(1)	0.227(1)	17.4(3)	6.95(4)	1.106(4)
		0.0091	48	0.1502(9)	0.0243(2)	0.194(2)	21.3(4)	7.21(4)	1.166(7)
	2.50	0.0233	28	0.2584(9)	0.0393(3)	0.328(2)	10.0(2)	7.23(3)	1.100(8)
		0.0178	36	0.2106(5)	0.0332(2)	0.267(2)	13.5(3)	7.58(2)	1.194(8)
		0.0141	40	0.1800(7)	0.0282(1)	0.227(2)	18.2(3)	7.20(3)	1.128(6)
		0.0114	48	0.1571(6)	0.0249(1)	0.202(1)	22.4(2)	7.54(3)	1.195(7)

Table 3. Data used for the chiral-continuum extrapolations. The temporal extent of the lattices were always twice L/a .